Desalination and Water Treatment
www.deswater.com

doi: 10.1080/19443994.2014.1000977

56 (2015) 3590–3598
December

Taylor & Francis
Taylor & Francis Group

High flux microfiltration membranes with silver nanoparticles for water disinfection

Aline Marques Ferreira[a], Érica Barbosa Roque[a], Fabiana Valéria da Fonseca[a,*], Cristiano Piacsek Borges[b]

[a]*School of Chemistry, Federal University of Rio de Janeiro, 21941-972, Rio de Janeiro, Brazil,*
emails: aferreira@peq.coppe.ufrj.br (A.M. Ferreira), ericabroque@yahoo.com.br (É.B. Roque), fabiana@eq.ufrj.br (F.V.da. Fonseca)
[b]*Chemical Engineering Program—COPPE, Federal University of Rio de Janeiro, 21941-972, Rio de Janeiro, Brazil,*
email: cristiano@peq.coppe.ufrj.br

Received 15 July 2014; Accepted 9 December 2014

ABSTRACT

Biofouling has a negative impact on the membrane water treatment since it reduces permeability, increases energy costs, and decreases the lifetime of the membranes. To minimize biofouling microfiltration (MF), polyethersulfone (PES) membranes were prepared by phase inversion method, and silver nanoparticles (AgNps) were synthesized by chemical reduction and incorporated into these MF membranes. Membranes with different pore size and porosity were selected and the presence of silver in the transversal section was confirmed. The antibacterial properties were analyzed against *Pseudomonas fluorescens* by the inhibition zone method after 24 and 96h of incubation and also by the bacterial count method. It was observed an inhibition ring of 20–30% of the sample diameter only around the membranes containing AgNps, indicating the suppression of micro-organism activity nearby the membrane. The permeate was analyzed using Colilert methodology to count the total number of coliforms. The coliform retention was 99.9 and 99.999% for membranes without and with AgNps, respectively. These results confirm the bactericide properties of the PES–AgNps membranes and their great potential in application for water treatment.

Keywords: Water disinfection; Microfiltration; Membranes; Biofouling; Antibacterial; Silver nanoparticles

---

1. Introduction

Microfiltration (MF) process shows a growing market for water disinfection, being estimated in 1.6 billions of dollars in 2013, and expected to grow up to 1.8 billions of US dollars in 2015 [1]. However, this process is limited by fouling and biofouling of the membrane, which reduces the permeate flux. Membrane biofouling results from the accumulation of organics, biofilm formation, and regrowth of micro-organisms on the membrane surface [2]. Common treatments to prevent or remove biofouling include the use of oxidative disinfectants or UV irradiation to

---

*Corresponding author.

Presented at the IX Ibero-American Congress on Membrane Science and Technology (CITEM 2014)
25–28 May 2014, Santander, Spain

reduce nutrients in the feed stream, clean-in-place to remove mature biofilm [3], and membrane surface modification to minimize biofilm growth [4–7].

New membranes with higher resistance to flux decline are a growing area of research and investment. Nanotechnology is one of the main approaches to develop membranes with unique surface properties. For instance, the use of silver nanoparticles (AgNps) can reduce micro-organism growth and, consequently, the membrane biofouling. Furthermore, presence of AgNps in MF membranes improves the disinfection of the permeate, allowing the use of membranes with high porosity and permeability. Membranes with these characteristics could be applied in several applications, including water treatment in food and pharmaceutical industries. Reduction of biofilm formation in membrane bioreactors for wastewater treatment and reuse it is another possibility.

Many methods exist to synthesize AgNps such as, chemical reduction of transition metal salts; thermal, photochemical, or sonochemical decomposition; metal vapor synthesis; and electrochemical reduction. Chemical reduction is the most widely used method to synthesize AgNps [8].

Silver AgNps have distinctive physico–chemical properties such as electrical and thermal conductivity, surface-enhanced Raman scattering, chemical stability, catalytic activity, and non-linear optical behavior [9]. Furthermore, AgNps act as antibacterial agents against a broad spectrum of micro-organisms [10].

The most accepted mechanism for water disinfection is the interaction of silver ions with thiol groups in proteins, resulting in inactivation of enzymes and production of reactive oxygen species (ROS). It is also shown that AgNps prevent DNA replication and affect the structure and permeability of the cell membrane. On the other hand, no evidence has been found on the toxicity of AgNps on human [11].

Some researchers reported the combination of polymeric membranes with biocides as silver AgNps. For instance, AgNps have been incorporated into membranes of different materials such as polysulfone [12,13], polyethersulfone (PES) [14,15], chitosan [16,17], and polyurethane [18,19].

This work synthesized silver AgNps by chemical reduction of silver nitrate ($AgNO_3$) in aqueous solution using polyvinylpyrrolidone (PVP) as a reducing and stabilizing agent. The MF membranes were prepared by inversion phase technique using PVP, PES, and dimethylacetamide (DMAc). The AgNps were incorporated in the MF membranes and the resulting membrane was evaluated for water disinfection.

2. Materials and methods

2.1. Materials

PES (PES, molecular weight 58,000 Da) was purchased from Basf. PVP (molecular weight 360,000 Da), silver nitrate ($AgNO_3$, 99.0%), and N,N-DMAc (DMA, 99.5%) were obtained from Sigma–Aldrich. PES and PVP were dried at 60 °C overnight and the other reagents were used as received. Ultrapure water used in all experiments was supplied by a Milli-Q system (Millipore). The agar plate used for bacterial incubation and the culture medium were purchased from Micromed and Sigma–Aldrich, respectively.

2.2. Preparation of PES membranes

PES and PVP were dissolved in DMA to form a homogeneous solution. The polymer solution was cast upon a glass plate with a casting knife and exposed to room atmosphere for a defined time before immersion in a DMA/water precipitation bath. Membranes were obtained by varying the composition of both the polymer solution and the immersion bath (Table 1).

2.3. Preparation of PES–AgNps membranes

An aqueous solution of silver nitrate (0.5%w/w) and PVP (2.0%w/w) were prepared to synthesize Ag-Nps. After the complete dissolution of PVP, $AgNO_3$ was added and stirred until complete dissolution occurred. The resulting solution was sonicated for 15 min to promote the chemical reduction of silver. PVP acts as a reducing agent due to the presence of an electron donor group in its structure, as well as a protective agent to reduce particle aggregation, controlling the AgNps' size. The AgNps suspension was characterized by UV–vis spectrometer (UV–vis Analyst-1803), and the absorption spectra were measured in the wavelength region from 200 to 600 nm. The incorporation of silver AgNps in selected PES membranes was carried out through dead-end filtration of the AgNps solution.

2.4. Membrane characterization

All synthesized membranes were characterized by Scanning Electron Microscope (SEM), (FEI Company Quanta 200), observing their surface and cross-section. Analysis of silver present on the membrane was conducted using energy dispersive X-ray spectrometer (Oxford Instruments) coupled to SEM.

The permeation properties of the membranes were evaluated in a cross-flow filtration system, using a

Table 1
Membrane preparation conditions

Membrane code	Polymer solution composition (%w/w) PES	PVP	DMA	Precipitation bath composition (v/v) DMA/water	Exposure time before immersion (s)
M1	11	11	78	50/50	15
M2	11	11	78	60/40	15
M3	11	11	78	70/30	15
M4	11	11	78	80/20	15
M5	9	9	82	60/40	15
M6	15	7.5	77.5	80/20	100

membrane effective area of 72 cm^2 and pure water. The transmembrane pressure varied from 0.5 to 1.0 bar, and the water permeability ($\mathrm{L\,h^{-1}\,m^{-2}\,bar}$) was obtained after stabilization of the permeate flux.

2.5. Antibacterial activity

The antibacterial properties of the AgNps membranes were investigated by the inhibition zone method. The Gram-negative species, *P. fluorescens* (ATCC 13525), was used as test micro-organism. The culture was grown overnight to achieve an optical density (OD_{600}) of 0.3, corresponding to approximately 10^5–10^6 $\mathrm{CFU\,mL^{-1}}$ of tested bacteria [20]. Aliquots (50 μL) of the bacterial suspension were spread with Drigalski spatel in agar plates, sterilized by ultraviolet radiation for 15 min before the experiment.

The membranes were cut into discs with a diameter of 20.0 mm and kept in contact with the agar surface at 37°C. The inhibition zone formed after 24 and 96 h served as an indicator of the antibacterial activity, and was recorded by a digital camera. The inhibition halo was expressed by the ratio between the membrane diameter and the halo diameter, according to Eq. (1).

$$\%\ \text{diameter increment} = \left[1 - \left(\frac{\text{membrane diameter}}{\text{total diameter}}\right)\right] \times 100 \tag{1}$$

Antibacterial effectiveness was also verified by filtration of an aqueous solution with 10^5 $\mathrm{CFU\,mL^{-1}}$ of *P. fluorescens*, using PES–AgNps and PES membranes. The membrane performance was determined in terms of the logarithmic reduction value (LRV) and retention (% *R*), according to Eqs. (2) and (3).

$$\mathrm{LRV} = \log_{10}\left(\frac{c_\mathrm{f}}{c_\mathrm{p}}\right) \tag{2}$$

$$\%\ R = (1 - 10^{-\mathrm{LRV}}) \times 100 \tag{3}$$

where, C_f and C_p are the bacterial concentrations in the feed and permeate streams, respectively.

3. Results

3.1. Characterization of AgNps suspension

In general, particles in nanoscale tend to have a spherical shape and UV–vis absorption due to the resonant excitation of plasma oscillations [21,22]. It is also known that the UV–vis absorption spectrum of silver AgNps is red-shifted for larger particle size. Conversely, smaller wavelength absorption corresponds to AgNps with smaller size. Furthermore, the presence of particle aggregates corresponds to a peak at a longer wavelength [23,24].

Fig. 1 shows the UV–vis absorption spectrum of the AgNps suspension. It may be observed that a well-defined plasmon band centered at about 280–300 nm, indicates AgNps. According to the previous results reported in literature [25,26], it is an indication of AgNps with an average diameter around 5 nm.

3.2. Membrane characterization

3.2.1. Membrane morphology

Membranes were prepared with different conditions to obtain a variety of morphologies, pore size, and permeabilities, allowing the investigation of their effect on AgNps fixation on the membrane, as well as the effectiveness in water purification. Fig. 2 portrays

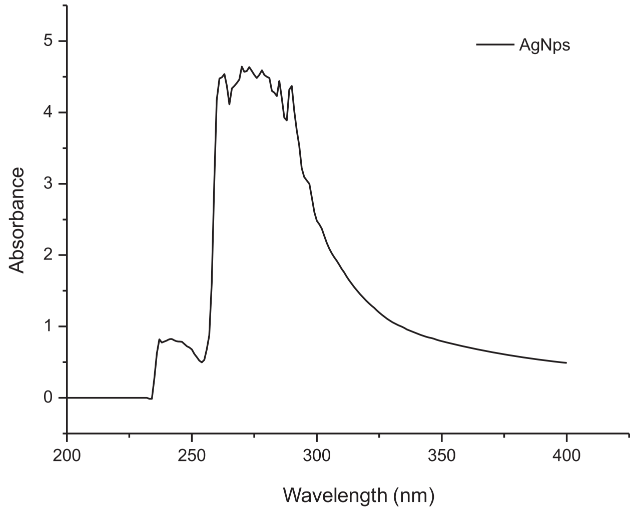

Fig. 1. UV–vis absorption spectrum of silver AgNps suspension.

SEM photomicrographs of the surface of the membranes M1, M2, M3, and M4, which were prepared from the same polymer solution but immersed in different precipitation baths (Table 1). It may be noted that there is an increase in the surface porosity with solvent (DMA) concentration in the precipitation bath, as a consequence of slower solvent–non-solvent mass exchange. This effect leads to lower polymer concentration at the onset of precipitation, favoring growth of the polymer lean phase and larger pores.

The cross-section of the membranes is also affected by increasing the solvent concentration in the precipitation bath. As it can be seen in Fig. 3, with lower solvent concentration in the precipitation bath, the membrane cross-section presents elongated macrovoids (Fig. 3(a) and (b)). However, addition of DMA solvent in the precipitation bath changes the membranes' morphology to sponge like with interconnected pores. As discussed by Machado et al. [27] the cross-section morphology is influenced by the onset of

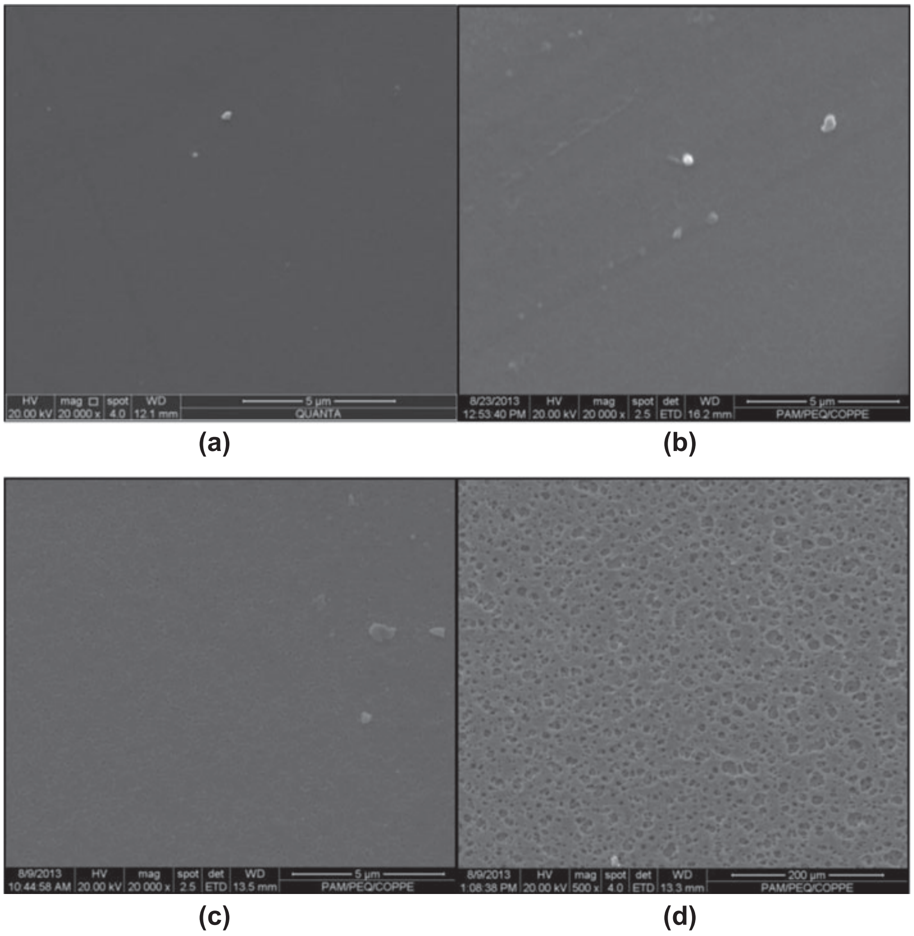

Fig. 2. SEM photomicrographs of membrane surface: (a) M1, (b) M2, (c) M3, and (d) M4.

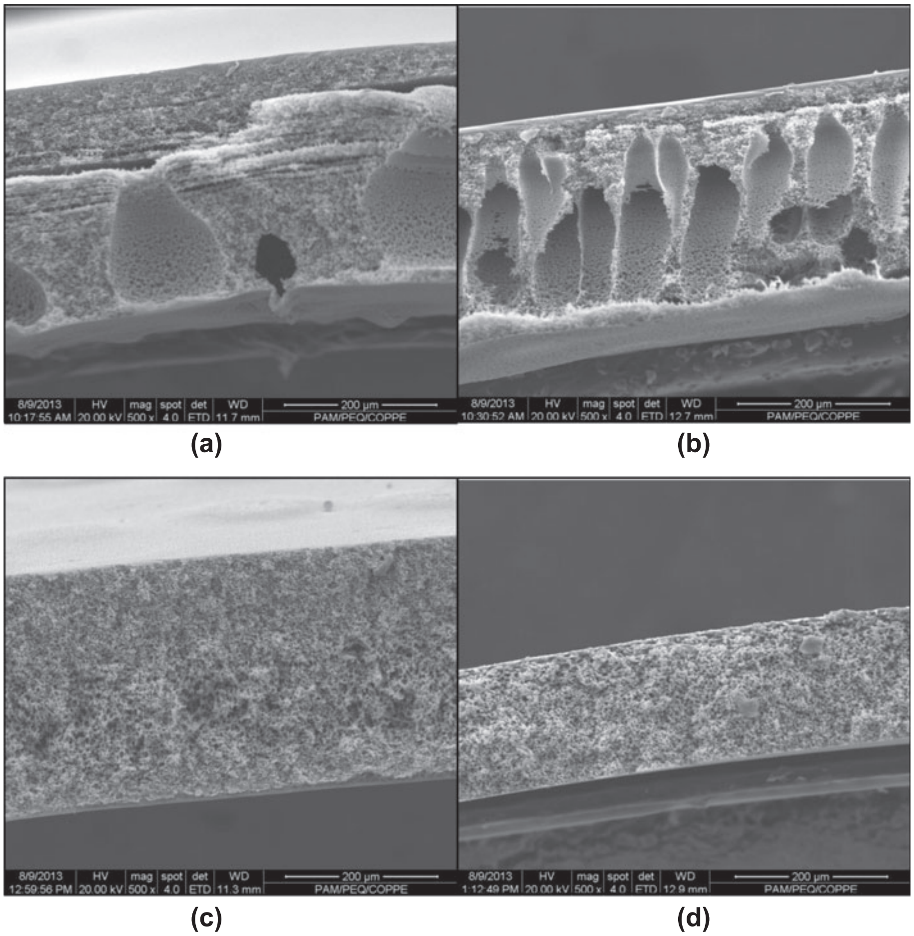

Fig. 3. SEM photomicrographs of membranes cross-section: (a) M1, (b) M2, (c) M3, and (d) M4.

precipitation in the top layer of the polymer solution. An instantaneous precipitation creates a denser top layer, reducing the mass exchange in the polymer solution beneath it, which favors the growth of the polymer lean phase and formation of macrovoids. On contrary, slower precipitation near the interface between the polymer solution and the precipitation bath intensifies solvent and non-solvent mass exchange in deeper regions of the incipient membrane, reducing the growth of the polymer lean phase.

The membrane M6 was prepared from a solution with higher polymer concentration, but allowing longer exposition to the environment before immersion. Fig. 4 shows the photomicrographs of the surface (Fig. 4(b)) and cross-section (Fig. 4(c)) of this membrane. During the exposition period, water vapor is absorbed by the solution, approximating it to the phase separation region, keeping the polymer concentration at low values. This condition favors the growth of the polymer lean phase and increase in the pore size.

The membrane M5 was prepared using lower polymer concentration in the solution, 15 s of exposition time before immersion in the precipitation bath and an intermediate concentration of DMA solvent in this bath. The morphology of the membrane cross-section, as expected, shows larger macrovoids.

3.2.2. *Presence of AgNps in the membrane*

The AgNps suspension was filtrated using different prepared membranes to fix the AgNps in the membrane pores for further evaluation of their antibacterial effectiveness. The Energy Dispersive Spectroscopy (EDS) spectra confirmed the presence of silver AgNps in all membrane cross-sections analyzed. Fig. 5 shows the spectra of membranes M3 and M6,

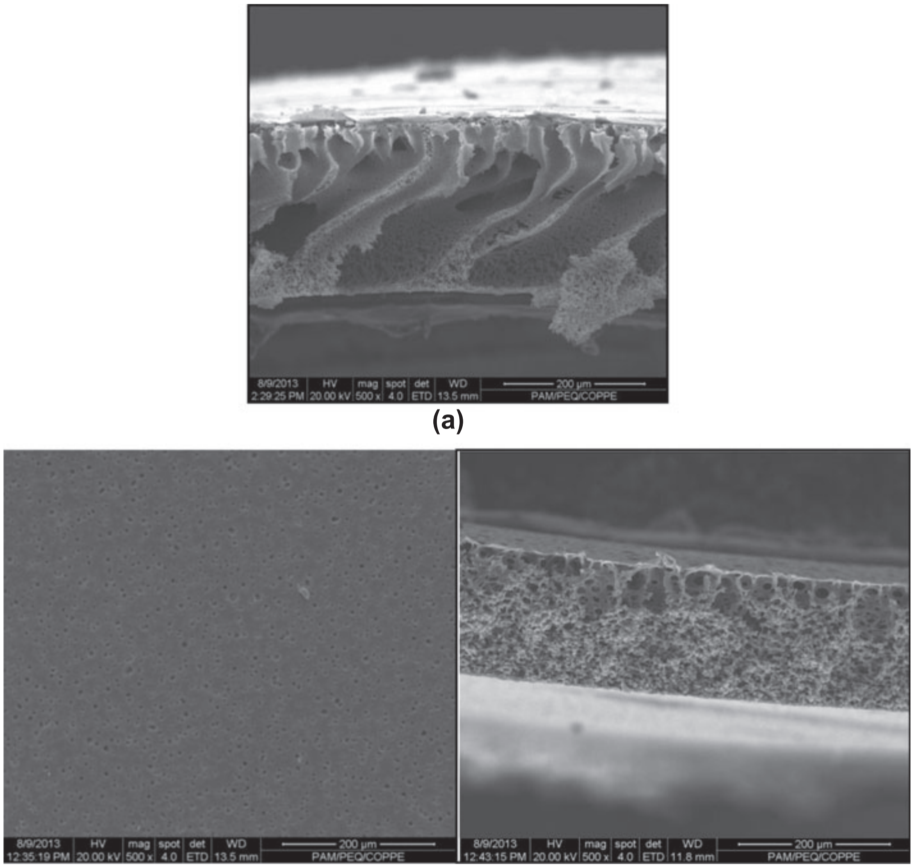

(a)

(b) (c)

Fig. 4. SEM photomicrographs of membranes M5 (a), M6 surface (b), and M6 cross-section (c).

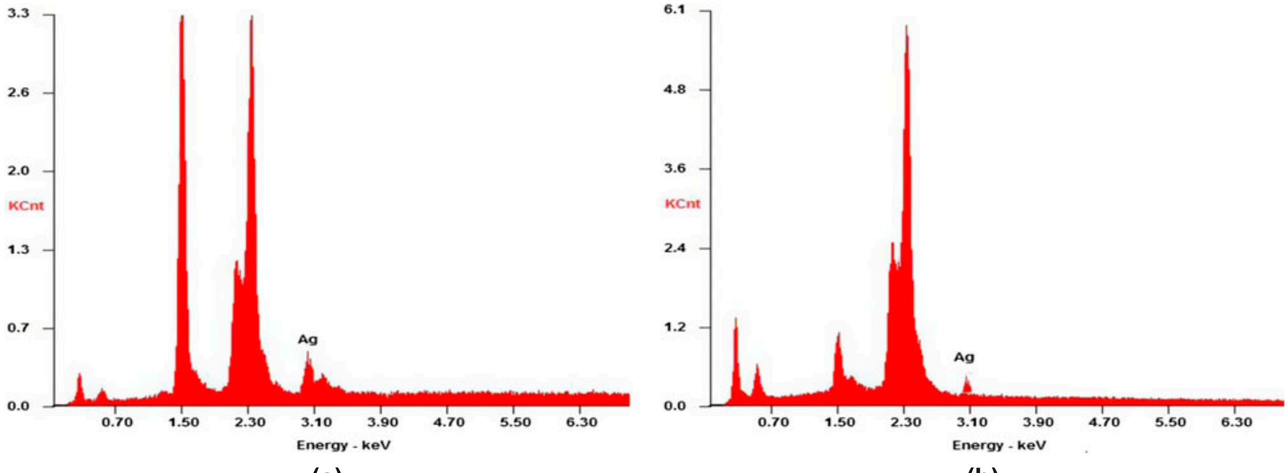

(a) (b)

Fig. 5. EDS spectra of (a) M3-AgNps and (b) M6-AgNps.

showing a peak relative to silver. It should be emphasized that these membranes have very different pore size and morphologies, indicating that AgNps are capable to adhere on the surface of PES/PVP membranes. To explain the fixation of AgNps in the membranes one should consider the amphiphilic

Table 2
Water permeability of PES membranes

Membrane	Pure water permeability ($\mathrm{L\,h^{-1}\,m^{-2}\,bar^{-1}}$)
M1	14.3
M2	230.7
M3	371.0
M4	11,017.0
M5	162.0
M6	3,051.0

nature of PVP, which is preferentially located at membrane surface after the polymer solutions' precipitation. Additionally, SEM photomicrographs reveal that the pores are interconnected, exhibiting high tortuosity. Hence, permeation of a solution with Ag colloidal particles through the membranes will promote inertial collisions of the particles with the membrane wall, and the physical–chemical properties of the membrane surface should favor AgNps adhesion.

3.2.3. Water permeability

The water permeability was determined using pure water and transmembrane pressure varying from 0.5 to 1.0 bar. Table 2 shows the water permeability of all PES membranes prepared in this work. The water permeability increases from membrane M1 to M4, which correlates with higher pore size and porosity as observed by SEM analysis. Membranes M5 and M6 which were prepared, respectively, at lower polymer concentration or longer exposition time, presented intermediated values of water permeability as a function of their pore size and overall porosity. Despite the large macropores observed in membrane M5, the pore size at its surface is smaller than those observed in membranes prepared from solution with higher polymer concentration. Once again, it may be a consequence of the precipitation onset, which is influenced by the solvent–non-solvent exchange.

3.3. Antibacterial activity

The antibacterial performance of the membranes was investigated by inhibition zone method that employed *P. fluorescens* as the test micro-organism. The membranes were kept on the medium with the bacteria and were incubated at 37°C. The membrane M1 without AgNps was used as a blank. All the membranes with AgNps showed antibacterial effect against *P. fluorescens* and Fig. 6 shows photographs of the membranes M1, M5, and M6 in agar plate after 24 and 96 h.

One may observe in Fig. 6(a) clear inhibition ring around PES–AgNps membranes. On the other hand, the membrane without silver AgNps was completely covered by the growth of *P. fluorescens* (Fig. 6(a)). The membrane M1 has the lowest pore size and, probably, AgNps was preferentially located at the outer surface, changing the membrane color and increasing the inhibition zone. The relative diameter increment values were used to quantify the inhibition effect and are reported in Table 3.

These results clearly indicate that AgNps incorporation in the membranes can effectively achieve antibacterial effect. Following several authors, the inhibition of micro-organism growth by AgNps could occur by different mechanisms. One possibility is that silver ions interact with thiol groups in proteins, resulting in inactivation of respiratory enzymes and leading to the production of reactive oxygen species that could lead to the damage or even the death of

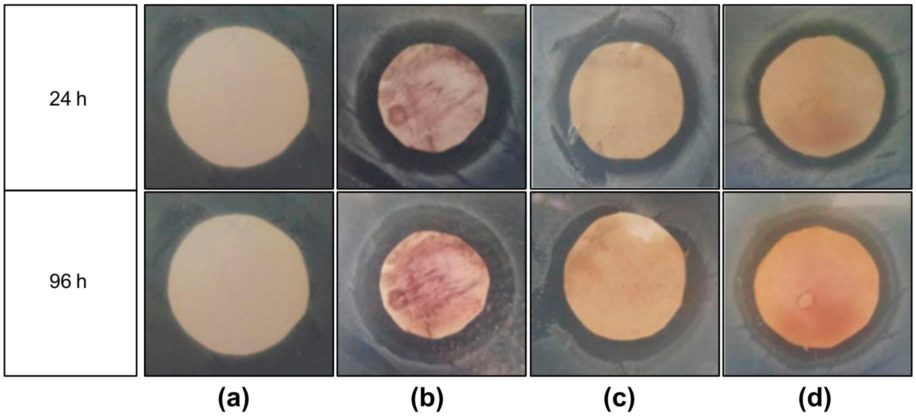

Fig. 6. Photographs of membranes after 24 or 96 h in contact with agar with *P. fluorescens*. (a) M1, (b) M1-AgNps, (c) M6-AgNps, and (d) M5-AgNps. The parts that are darker showed inhibition, while the lighter parts did not.

Table 3
Relative diameter increment values

Membrane	% Diameter increment (24 h)	% Diameter increment (96 h)
M1	0	0
M1-AgNps	30.5	31.6
M5-AgNps	21.3	25.6
M6-AgNps	19.2	24.8

Table 4
Permeate analysis using Colilert methodology

Permeate sample	Total coliforms (MPN 100 mL^{-1}) in the permeate	LRV	Microorganism retention (%)
M1	1.79×10^2	3.02	99.9
M1-AgNps	3.0	4.80	99.999
M5	1.87×10^2	3.00	99.9
M5-AgNps	1.0	5.27	99.999

Note: Total coliforms in the feed solution (MPN.100 mL^{-1}): 1.87×10^5.

bacterial cells [11,28–30]. Other possibility is related to Ag$^+$ ions that prevent DNA replication. Thirdly, AgNps can also be attached to the membrane cell surface, affecting its structure and permeability [29–32].

The antibacterial activity was also evaluated during permeation of a feed solution containing *P. fluorescens*. The permeate stream was analyzed, and the LRV and the coliform retention are shown in Table 4.

The feed solution showed substantial growth of bacteria, 1.87×10^5MPN. 100 mL^{-1}. However, a high retention of micro-organisms was observed in the permeate, higher than 99.9%. For membranes containing AgNps, the retention was as high as 99.999%, corresponding to LRV close to five. It is interesting to observe that the highest retention values were observed for the membrane with higher pore size and permeability. Hence, one may conclude that AgNps effectively allows the use of membranes with bigger pores, keeping the permeate quality. These results confirm the bactericide properties of the MF membranes containing silver AgNps and the great potential in application for water treatment.

4. Conclusions

In this work, membranes were prepared with different morphologies, pore size, and water permeability. These membranes were used to evaluate incorporation of silver AgNps by dead-end filtration. The presence of silver peak in all membranes was observed by SEM/EDS, indicating that AgNps could adhere to the membrane pore surface. The membranes with AgNps exhibit antibacterial effect, as observed by the inhibition zone method and reduces the microorganism contamination in the permeate stream.

Membranes with small pore size at outer surface do not allow silver AgNps to permeate through the membrane, increasing their concentration at the outer surface of the membrane. AgNps can enter inside the cross-section of membranes with bigger pore size. The presence of AgNps in these membranes improves disinfection of the permeate, allowing the use of membranes with high porosity and permeabilities for water treatment.

References

[1] BCC RESEARCH. BCC Research, 2011. Available from: http://www.bccresearch.com.

[2] N. Hilal, V. Kochkodan, L. Al-Khatib, T. Levadna, Surface modified polymeric membranes to reduce (bio)fouling: A microbiological study using *E. coli*, Desalination 167 (2004) 293–300.

[3] A. Dror-Ehre, A. Adin, H. Mamane, Control of membrane biofouling by silver nanoparticles using *Pseudomonas aeruginosa* as a model bacterium, Desalin. Water Treat. 48 (2012) 130–137.

[4] C.X. Liu, D.R. Zhang, Y. He, X.S. Zhao, R. Bai, Modification of membrane surface for anti-biofouling performance: Effect of anti-adhesion and anti-bacteria approaches, J. Membr. Sci. 346 (2010) 121–130.

[5] R. Malaisamy, D. Berry, D. Holder, L. Raskin, L. Lepak, K.L. Jones, Development of reactive thin film polymer brush membranes to prevent biofouling, J. Membr. Sci. 350 (2010) 361–370.

[6] D. Rana, T. Matsuura, Surface modifications for antifouling membrabes, Chem. Rev. 110 (2010) 2448–2471.

[7] F. Razi, I. Sawada, Y. Ohmukai, T. Maruyama, H. Matsuyama, The improvement of antibiofouling efficiency of polyethersulfone membrane by functionalization with zwitterionuc monomers, J. Membr. Sci. 401–402 (2012) 292–299.

[8] A. Roucoux, J. Schulz, H. Patin, Reduced transition metal colloids: A novel family of reusable catalysts? Chem. Rev. 102 (2002) 3757–3778.

[9] W. Ma, D. Zhong, H. Han, P. Wang, A review: Inhibition of Ag NPs on wastewater treatment, Desal. Water Treat. 51 (2013) 1–6.

[10] G. Zhao, E. Stevens Jr., Multiple parameters for the comprehensive evaluation of the susceptibility of *Escherichia coli* to the silver ion, Biometals 11 (1998) 27–32.

[11] J.R. Morones, J.L. Elechiguerra, A. Camacho, K. Holt, J.B. Kouri, J.T. Ramírez, M.J. Yacaman, The bactericidal effect of silver nanoparticles, Nanotechnology 16 (2005) 2346–2353.

[12] K. Zodrow, L. Brunet, S. Mahendra, D. Li, A. Zhang, Q. Li, P.J.J. Alvarez, Polysulfone ultrafiltration membranes impregnated with silver nanoparticles show improved biofouling resistance and virus removal, Water Res. 43 (2009) 715–723.

[13] J.S. Taurozzi, H. Arul, V.Z. Bosak, A.F. Burban, T.C. Voice, M.L. Bruening, V.V. Tarabara, Effect of filler incorporation route on the properties of polysulfone-silver nanocomposite membranes of different porosities, J. Membr. Sci. 325 (2008) 58–68.

[14] H. Basri, A.F. Ismail, M. Aziz, K. Nagai, T. Matsuura, M.S. Abdullah, B.C. Ng, Silver-filled polyethersulfone membranes for antibacterial applications–Effect of PVP and TAP addition on silver dispersion, Desalination 261 (2010) 264–271.

[15] M. Zhang, K. Zhang, B. De Gusseme, W. Verstraete, Biogenic silver nanoparticles (bio-Ag_0) decrease biofouling of bio-Ag_0/PES nanocomposite membranes, Water Res. 46 (2012) 2077–2087.

[16] Y.H. Tee, B. Bhattacharyya, Chitosan Membranes with nanoparticles for remediation of chlorinated organics, in: N.N. Li, A.G. Fane, W.S.W. Ho, T. Matsuura (Eds.), Chapter 8: In Advanced Membrane Technology and Applications, Wiley, New Jersey, NJ, 2008.

[17] R. Yoksan, S. Chirachanchai, Silver nanoparticle-loaded chitosan–starch based films: Fabrication and evaluation of tensile, barrier and antimicrobial properties, Mater. Sci. Eng. C. 30 (2010) 891–897.

[18] P. Jain, T. Pradeep, Potential of silver nanoparticle-coated polyurethane foam as an antibacterial water filter, Biotechnol. Bioeng. 90 (2005) 59–63.

[19] N.T.P. Phong, N.V.K. Thanh, P.H. Phuong, Fabrication of antibacterial water filter by coating silver nanoparticles on flexible polyurethane foams, J. Phys. 187 (2009) 1–8.

[20] M. Pereda, A.G. Ponce, N.E. Marcovich, R.A. Ruseckaite, J.F. Martucci, Chitosan-gelatin composites and bi-layer films with potential antimicrobial activity, Food Hydrocolloids 25 (2011) 1372–1381.

[21] J.D. Guingab, B. Lauly, B.W. Smith, N. Omenetto, J.D. Winefordner, Stability of silver colloids as substrate for surface enhanced Raman spectroscopy detection of dipicolinic acid, Talanta 74 (2007) 271–274.

[22] J.J. Mock, M. Barbic, D.R. Smith, D.A. Schultz, S. Schultz, Shape effects in plasmon resonance of individual colloidal silver nanoparticles, J. Chem. Phys. 116 (2002) 6755–6759.

[23] S.Y. Lee, H.J. Kim, R. Patel, S.J. Im, J.H. Kim, B.R. Min, Silver nanoparticles immobilized on thin film composite polyamide membrane: Characterization, nanofiltration, antifouling properties, Polym. Adv. Technol. 18 (2007) 562–568.

[24] N. Kim, C. Kim, Y. Lee, Effect of the polymer matrix on the formation of silver nanoparticles in polymer-silver salt complex membranes, J. Polym. Sci., Part B: Polym. Phys. 44 (2006) 1168–1178.

[25] Z.H. Mbhele, M.G. Salemane, C.G.C.E. Van Sittert, J.M. Nedeljkovic, V. Djokovic, A.S. Luyt, Fabrication and characterization of silver–polyvinyl alcohol nanocomposites, Chem. Mater. 15 (2003) 5019–5024.

[26] V.V. Vukovic, J.M. Nedeljkovic, Surface modification of nanometer-sclae silver particles by imidazole, Langmuir 9 (1993) 980–983.

[27] P.S.T. Machado, A.C. Habert, C.P. Borges, Membrane formation mechanism based on precipitation kinetics and membrane morphology: Flat and hollow fiber polysulfone membranes, J. Membr. Sci. 155(2) (1999) 171–183.

[28] J. Huang, G. Arthanareeswaran, K. Zhang, Effect of silver loaded sodium zirconium phosphate (nanoAgZ) nanoparticles incorporation on PES membrane performance, Desalination 285 (2012) 100–107.

[29] Y. Matsumura, K. Yoshikata, S. Kunisaki, T. Tsuchido, Mode of bactericidal action of silver zeolite and its comparison with that of silver nitrate, Appl. Environ. Microbiol. 69 (2003) 4278–4281.

[30] Q.L. Feng, J. Wu, G.C. Chen, F.Z. Cui, T.N. Kim, J.O. Kim, A mechanistic study of the antibacterial effect of silver ions on *Escherichia coli* and *Staphylococcus aureus*, J. Biomed. Mat. Res. 52 (2000) 662–668.

[31] I. Sondi, B. Salopek-Sondi, Silver nanoparticles as antimicrobial agent: A case study on *E. coli* as a model of Gram-negative bacteria, J. Colloid Interface Sci. 275 (2004) 177–182.

[32] O. Choi, K.K. Deng, N. Kim, L. Ross Jr., R.Y. Surampalli, Z. Hu, The inhibitory effects of silver nanoparticles, silver ions, and silver chloride colloids on microbial growth, Water Res. 42 (2008) 3066–3074.